IJE TRANSACTIONS C: Aspects Vol. 37 No. 03, (March 2024) 484-495

International Journal of Engineering

Journal Homepage: www.ije.ir

Investigation of Laser Cutting of Thin Polymethyl Methacrylate Sheets by Response Surface Methodology

M. Safari*, J. Joudaki, M. Rezaei

Department of Mechanical Engineering, Arak University of Technology, Arak, Iran

PAPER INFO

Paper history:
Received 27 August 2023
Received in revised form 26 October 2023
Accepted 31 October 2023

Keywords:
Laser Cutting
Polymethyl Methacrylate
Kerf Geometry
Surface Roughness
Response Surface Methodology

ABSTRACT

Laser cutting is a precise, powerful, and low-cost tool for cutting different sheets of metals and polymers. The literature survey shows that the quality of cutting (surface roughness and kerf geometry) is a sophisticated parameter and conventional approaches cannot describe the quality of cutting for thin sheets of polymers very well. Statistical tools can help to interpret the effect of process variables. In this article, the laser cutting of Polymethyl methacrylate (PMMA) is experimentally investigated. The effect of process variables of laser cutting including the scanning speed, laser power, and laser beam diameter on the kerf width and surface roughness by Response Surface Methodology design investigated. The results revealed that increasing the laser power leads to increasing the surface roughness and decreasing the taper angle, while the kerf width at the top and bottom surface of the sheet decreases at first, then increases (for higher laser power than 90W). Also, increasing the scanning speed causes increasing surface roughness while the taper angle and the kerf width at the top and bottom surface increase at first, then it decrease. By increasing the laser beam diameter, the surface roughness will increase while the taper angle and the kerf width at the top and bottom surface decrease at first and then increase. The sophisticated effect of the main process variables and their interactions determines that finding the optimum condition of process parameters is hard and multi-objective optimization approaches are needed to find local minimum surface roughness and kerf geometry.

doi: *10.5829/ije.2024.37.03c.05*

1. INTRODUCTION

Laser cutting is a non-contact process that produces precise cutting along a defined curve with minimum heat affected zone (HAZ) and minimum distortion of the sheet while no external load is applied to the sheet. This process is mostly utilized for the precise cutting of metals, especially steel alloys. However, in recent years, the use of low-power laser beams to cut different types of polymers has spread. The laser cutting process can be carried out for different purposes. Cutting and producing a blank workpiece is the most convenient. But by performing the cutting at low laser power, microchannel with very low surface roughness (as low as 110 nm) can be fabricated for microfluidic studies (1-3).

One of the most convenient polymers is Polymethyl Methacrylate (PMMA). PMMA is one of the most appropriate thermoplastics for laser cutting. PMMA has a high melting point (160°C) and high absorptivity of the laser wavelength, 2.914 GPa elastic modulus, 79.16 MPa tensile strength, and 0.40 strain at failure (4). Choudhury and Shirley (5) studied the quality of surface roughness, formation of heat affected zone (HAZ), and dimensional accuracy during laser cutting of different materials (polymethyl methacrylate (PMMA), polypropylene (PP), and polycarbonate (PC)). The results show that surface roughness is improved in laser cutting of PMMA polymer compared to PP and PC. The width of HAZ decreased in PMMA compared to PP and PC polymers. Moreover, similar dimensional accuracy was achieved despite different material properties.

Eltawahni et al. (6) studied the kerf width variation and surface roughness variation during the laser beam cutting of ultra-high molecular weight polyethylene (UHMWPE) material. A design of experiments has been done and the effect of process variables including laser

*Corresponding Author Email: m.safari@arakut.ac.ir (M. Safari)

Please cite this article as: Safari M, Joudaki J, Rezaei M. Investigation of Laser Cutting of Thin Polymethyl Methacrylate Sheets by Response Surface Methodology. International Journal of Engineering, Transactions C: Aspects. 2024;37(03):484-95.

power, cutting speed, and focal point position is discussed by performing 17 different experiments. The levels of laser power were very high (800-1150 W) due to the property of UHMWPE. The results show that the kerf at the upper surface was reduced by decreasing the laser power and increasing the cutting speed and the focal position. In addition, the kerf at the bottom decreases by decreasing the laser power and focal position and increasing the cutting speed. Also, Eltawahni et al. (7) discussed the advantage of CO_2 laser for cutting four different thicknesses of PMMA by employing a Box-Behnken design of the experiments.

Response Surface Methodology (RSM) and the Taguchi method are two of the approaches for the design of experiments (8-10). Khoshaim et al. (11) investigated the laser cutting of PMMA sheets by a continuous CO_2 laser. A design of experiments based on Taguchi L18 design was planned and the effect of input variables (cutting speed, laser power, sheet thickness, and assisting gas pressure) on output variables responses has been investigated. The output variables of the study were kerf deviation, maximum surface roughness, heat-affected zone (HAZ), and rough area. Regression equations were derived according to the effectiveness of each process input. The results show that by increasing the laser power and gas pressure, the kerf deviation and roughness increase. The kerf deviation increases and the roughness decreases by increasing the cutting speed. The results show that for obtaining the best surface roughness and decreased HAZ, lower laser power, and higher cutting speed were experimentally implemented. Unfortunately, high kerf deviation is inevitable at higher cutting speeds. Elsheikh et al. (12)studied the formation of kerf during the cutting of PMMA by a pulsed CO_2 laser machine. The effect of process variables including cutting speed, laser power, assisted gas pressure, and sheet thickness was investigated using Taguchi L18 orthogonal array. Using the analysis of variance technique (ANOVA), the effect of process variables has been determined. The results show that the top and the bottom kerf widths decrease by increasing the laser power, cutting speed, and gas pressure. The kerf taper angle increases by increasing the cutting speed. The effect of laser power and gas pressure on the kerf taper angle is almost negligible. Increasing the thickness leads to a decrease in the top and the bottom kerf width and kerf taper angle. Genetic Algorithm (GA) and random vector functional link network with equilibrium optimizer (RVFL-EO) algorithm (13) were used to optimize the quality of cutting. Yang et al. (14) developed a combined strategy called the progressive Taguchi neural network model for assessing the kerf taper angle during laser cutting of PMMA sheets by combining the artificial neural network and Taguchi method. The results show that a higher precision can be obtained by the proposed method while the number of experiments decreased with using the L9 orthogonal array instead of the L18 or L27 orthogonal array.

Ninikas et al. (15) studied the influence of the cutting speed and laser power, and the position and orientation of the samples, on the dimensional accuracy and surface roughness of laser cutting of PMMA sheets. A mixed fractional factorial design (36 measurements) was carried out and the dimensional accuracy and surface roughness were measured. The ANOVA results showed that the cutting speed is the most influential process parameter for both dimensional accuracy and surface roughness. Also, the surface roughness improves and minimizes for samples aligned in the travel direction. Also, the authors proposed a neural network-based approach to predict the kerf geometry in laser cutting of PMMA sheets (16) and 3D-printed Polylactic Acid (PLA) (17). Varsi and Shaikh (18) studied the effect of process variables (power, cutting speed, and the number of passes) on the kerf taper angle during the drilling of cylindrical holes in PMMA sheets by the laser beam. The full factorial methodology was used for data analysis and the results show that the kerf taper angle decreases by increasing the laser power and number of passes and decreasing the cutting speed. Several researches have been done in the field of laser cutting. Mushtaq et al. (19) discussed the latest advances in laser cutting of polymers. Hashemzadeh et al. (20) also studied the effect of workpiece vibration in the vertical direction (parallel to the laser beam) at different frequencies. The thickness of the PMMA sheet was 6 mm and cutting was carried out by 70 W laser power. The results show that the laser beam cut through the depth at lower scanning speeds (in the range of 0.2 to 0.4 m/s) while a groove will be formed at higher scanning speeds (0.4 to 2 m/s). the depth of cut increases by increasing the vibration frequency. The authors also published research about the utilization of laser beams and their different applications in industries (21-23).

The literature survey shows that laser cutting is a complicated phenomenon and based on the attitude of the researchers it can be carried out in different ways. Each of the researchers specified some aspect of the cutting process that was novel. Analyzing the published research shows that some researchers only focused on the surface quality and improving it while others explored the kerf formation (width of the kerf, taper angle). However, parameters improving the surface roughness lead to higher kerfs and vice versa. The main challenge in the laser cutting of PMMA sheets is the different behavior of scanning speed and laser beam diameter at high and low laser power. The design of Experiments by RSM helps to find a second-order regression equation to assess the effect of parameters. In this research, the authors attempt to investigate the effect of influencing process variables to optimize the surface roughness and kerf geometry

simultaneously. In this article, the laser cutting of PMMA thin sheets (2.8 mm thickness) will be investigated by using a low power laser beam machine. A design of experiments according to RSM has been scheduled and the surface roughness and kerf width at the top and bottom of the surface was measured. The effect of process variables and their interactions will be discussed by ANOVA. The main difference between current work and other published research is the range of parameters and discussion about the effect of the interaction of process variables in laser cutting of thin sheets that has a negligible effect in laser cutting of thick sheets. Finally, a discussion about the optimization of parameters with different attitudes (cost function) will be added.

In this article, firstly an experiment planning will be carried out and the geometry of kerf due to laser cutting will be measured. Then, the effect of –process parameters and their interactions will be investigated by ANOVA and statistical tools of Minitab software. Finally, the optimization of the process variables will be carried out.

2. EXPERIMENTAL WORKS

The experimental works have been carried out on a PMMA sheet prepared by an approved supplier. The sheet thickness was 2.8 mm. The laser beam irradiated the surface of the sheet. Based on the literature survey, it was decided that the effect of three more important process variables (laser power, scanning speed, and laser beam diameter) will be investigated. For determining the levels of process parameter variation, some pre-tests have been carried out. The aim was to find proper process parameters that melt and cut the sheet without over-melting. In this way, the levels of process parameter variations are determined in Table 1. It should be noted that proper selection of the range of process variables is very important. For example, if the sheet did not cut under one of the designed tests, the statistical analysis cannot be completed and the regression equations cannot be obtained. In this circumstance, all of the implemented tests should be repeated with new levels of process variables which have considerable cost. So, some pre-tests have been carried out and the levels of parameters determined.

The important object in laser cutting is the effect of simultaneous variation of process parameters. For this purpose, the design of experiments (DOE) techniques have been utilized. Because the aim is the identification of the role of parameters, the RSM has been utilized. The list of experiments (15 tests) is shown in Table 2. The tests were determined according to the Box-Behnken approach in Minitab Software.

The laser beam was produced by a Ressi laser beam (RT1310U) machine which is a CO_2 source, continuous wave machine. The PMMA sheet was placed on the table

TABLE 1. The levels of process parameters variation in laser cutting of PMMA

Process Parameters	Value	Unit
Laser Power	72 90 108	W
Scanning Speed	10 20 30	mm/s
Laser Beam Diameter	0.2 0.6 1	mm

TABLE 2. List of experiments according to RSM

Run Order	Power (W)	Scanning speed (mm/s)	Beam diameter (mm)
1	90	30	0.2
2	90	10	0.2
3	72	10	0.6
4	90	30	1.0
5	72	20	1.0
6	90	20	0.6
7	90	20	0.6
8	90	10	1.0
9	108	20	0.2
10	108	30	0.6
11	108	10	0.6
12	90	20	0.6
13	72	20	0.2
14	108	20	1.0
15	72	30	0.6

of the laser machine and after irradiation of the laser beam for 40 mm length, the cutting process stopped and after moving the laser gun laterally, the next groove with new cutting parameters will be machined. Figure 1 shows a schematic view of the cutting cross-section of the laser beam. At ideal conditions, a square cross-section should be created but due to the small angular divergence of the laser beam, a trapezoidal cross-section will be formed. The kerf geometry consists of two parameters: the top kerf width (W_t) and the bottom kerf width (W_b). Therefore, the conical angle of the kerf (α) is defined as Equation 1.

$$a = \tan^{-1}\left(\frac{W_t - W_b}{2t}\right) \quad (1)$$

where t is the thickness of the sheet.

The roughness was measured by a SURFSCAN200 surface roughness tester machine. The probe of the roughness tester machine moves along a path on the surface and measures the profile of the surface. The average arithmetic roughness Ra is calculated by the

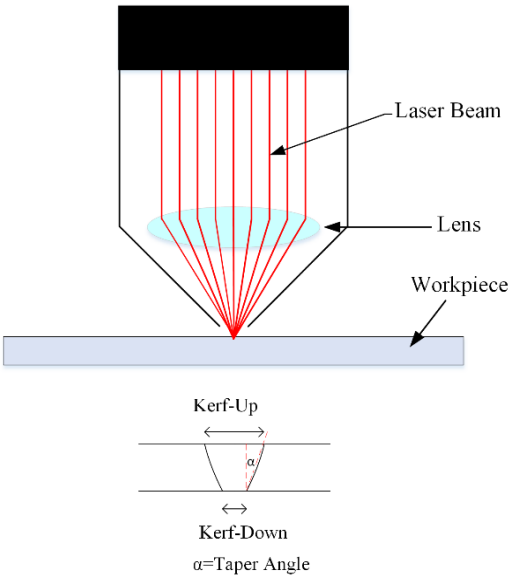

Figure 1. Schematic of laser beam kerf

machine and reported as the result of measurement. Some of the cutting of the PMMA sheet is shown in Figure 2(a). In addition, the cut specimens were observed by a DP73 OLYMPUS optical microscope, and the kerf width was measured by the calibrated software of OM. Figure 2(b) shows some images of kerfs (50X magnification). After that, the surface roughness was measured at three different locations along the laser travel direction, and the average of them is reported as the final result of the surface roughness. Figure 3 shows the surface roughness measurement apparatus. The resolution of the machine is 0.001 µm. The experiments were conducted in 2023 at the Laser Processing Laboratory of Arak University of Technology.

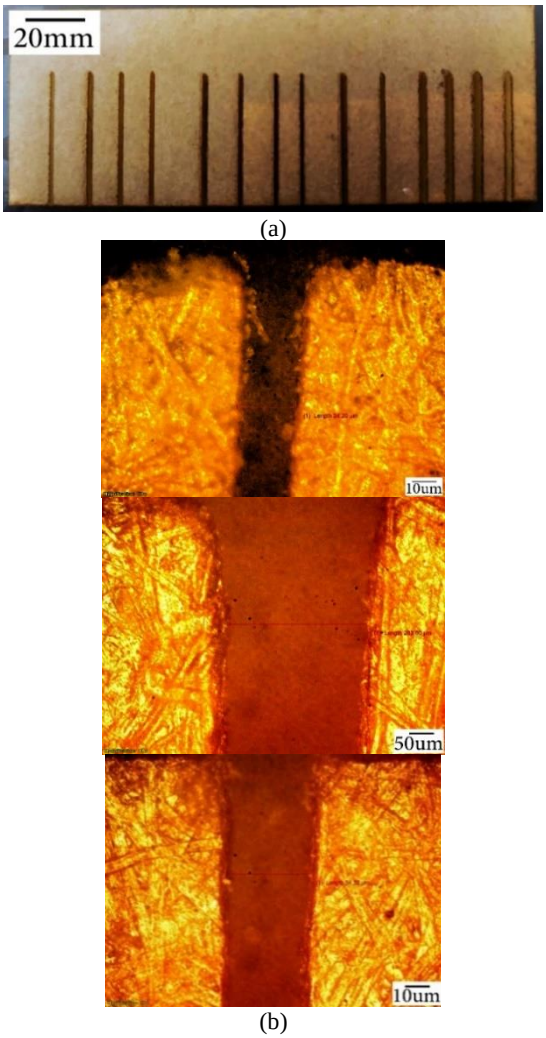

Figure 2. The laser cutting of PMMA sheet a) top view b) side view (observed by OM)

Figure 3. SURFSCAN200 roughness measurement machine

3. RESULTS AND DISCUSSION

3. 1. Surface Roughness Variation After measuring the width of the kerf and surface roughness, the analysis of results has been carried out by Minitab software. Table 3 shows the results of ANOVA for surface roughness designed based on response surface methodology. The P-Value column (less than 0.05) shows the significance or effectiveness of each process parameter. The results show that the scanning speed and beam diameter are influencing parameters and the power parameter is not affecting the surface roughness. Equation 2 shows the fitted equation for the prediction of surface roughness. The determination factor R^2 for surface roughness is 90.85 % which is a good quality curve fitting. Figure 4 shows the main effect plot for the roughness of the cut surface. As can be seen in Figure 4, the beam diameter is a very important parameter of the quality of roughness. Minimum surface roughness is obtained in 0.3 mm beam diameter and surface roughness is almost constant in the range of 0.2 to 0.4 mm. The

TABLE 3. ANOVA results for surface roughness

Source	DF	Adj SS	Adj MS	F-Value	P-Value
Model	7	15.5210	2.2173	9.93	0.004
Linear	3	12.4175	4.1392	18.54	0.001
Power (W)	1	0.2450	0.2450	1.10	0.330
Scanning Speed (mm/s)	1	1.3613	1.3613	6.10	0.043
Beam Diameter (mm)	1	10.8112	10.8112	48.42	0.000
Square	1	2.1910	2.1910	9.81	0.017
Beam Diameter (mm)*Beam Diameter (mm)	1	2.1910	2.1910	9.81	0.017
2-Way Interaction	3	0.9125	0.3042	1.36	0.330
Power (W)*Scanning Speed (mm/s)	1	0.2500	0.2500	1.12	0.325
Power (W)*Beam Diameter (mm)	1	0.6400	0.6400	2.87	0.134
Scanning Speed (mm/s)*Beam Diameter (mm)	1	0.0225	0.0225	0.10	0.760
Error	7	1.5630	0.2233		
Lack-of-Fit	5	0.6030	0.1206	0.25	0.908
Pure Error	2	0.9600	0.4800		
Total	14	17.0840			

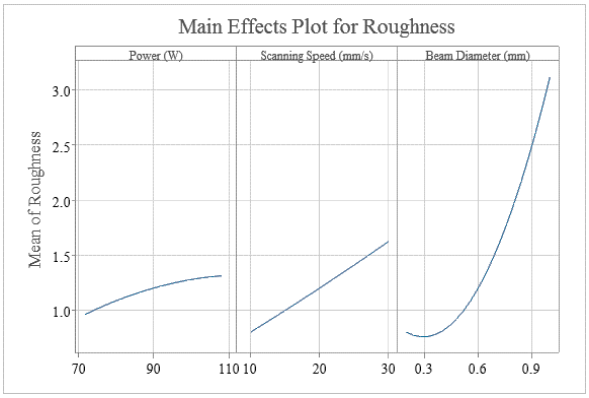

Figure 4. Main effect plot for surface roughness

surface roughness increases rapidly for beam diameters higher than 0.5 mm. The surface roughness increases by increasing the scanning speed (with a constant slope line). The laser power has the least effect on the surface roughness. The surface roughness increases with laser power too. Because all of the process parameters increase the surface roughness, the interaction of process parameters is always positive and increases the surface roughness. More details about the ANOVA results term can be found by Montgomery (24).

$$\begin{aligned} Roughness = & -0.27 + 0.0042P + 0.178S - 7.46D \\ & + 4.79D^2 - 0.00139P \times S \\ & + 0.0556P \times D - 0.0188S \times D \end{aligned} \quad (2)$$

A similar study was implemented by Huang et al. (3)on PMMA material. The thickness was 2 mm which is near the thickness of the current study. The surface roughness was reported in the range of 0.75 to 3 Ra surface roughness. The laser power was very low (15-45 W) and the surface roughness increased by increasing the laser power. However, the results of the current study show that better surface roughness can be obtained at higher laser power. The surface roughness also was in the range of 0.55 to 2.5 for scanning speed varying from 10 to 50 mm/s and the surface roughness increased by increasing the scanning speed linearly. However, the results of the current study show that better surface roughness can be obtained at higher scanning speeds. As can be seen, the trends are similar, but this study shows that laser beam diameter is a key factor (most influencing factor) on the surface roughness and a good quality surface can be obtained by decreasing the laser beam diameter. Huang et al. (3) studied the effect of process parameters (laser power and scanning speed) by varying one factor at a time and keeping constant the other parameters while RSM helps to better interpret the effect of main process parameters and their interactions.

3. 2. Kerf Width Variation The kerf width at the top and bottom surface behaves a little differently. Tables 4 and 5 show the ANOVA results for kerf width at the top (Kerf-up) and bottom (Kerf-down) surfaces. The results of ANOVA were illustrated as a graphical image in Figure 5 (Pareto chart). It is evident that the laser power and laser beam diameter are the influential process parameters and scanning speed is an unimportant parameter on the kerf width at the top surface. All of the square terms of process parameters influence process variables. The interaction of laser power with laser beam diameter and scanning speed with laser beam diameter are also important in process parameters on the kerf width of the top surface. As can be seen, the only insignificant process parameters are scanning speed and the interaction of scanning speed with laser power. The Pareto chart for the kerf width of the bottom surface shows that the square of laser power is the only significant process parameter and other process parameters, interactions, and squares are insignificant. Equations 3 and 4 show the regression equation for Kerf-up and Kerf-down width as a full quadratic equation. The determination factor R2 for Kerf-up and Kerf-down width is 98.72 and 82.32 % which shows that the equations can predict the kerf width at the top and bottom surface with adequate precision.

$$Kerf-up = 3830 - 67.96P + 22.64S - 2137D + 0.3375P^2 - 0.4674S^2 + 608.1D^2 - 0.1079P \times S + 13.48P \times D + 7.34S \times D \quad (3)$$

$$Kerf-Down = 1953 - 36.3P + 11.6S - 810D + 0.1880P^2 - 0.505S^2 + 342D^2 + 0.049P \times S + 2.76P \times D + 5.00S \times D \quad (4)$$

The main effect plot for Kerf-up and Kerf-down width is shown in Figure 6. The kerf width at the top surface decreases by increasing the laser power at first, then it increases such that the local minimum happens at about 90 W laser power and 0.6 mm beam diameter. The kerf width increases by increasing the scanning speed at first, then it decreases. The minimum kerf width at the top surface happens at 30 mm/s scanning speed. Similar

TABLE 4. ANOVA results for Kerf-up

Source	DF	Adj SS	Adj MS	F-Value	P-Value
Model	9	138877	15430.8	42.97	0.000
Linear	3	8650	2883.5	8.03	0.023
Power (W)	1	4248	4247.7	11.83	0.018
Scanning Speed (mm/s)	1	1489	1488.9	4.15	0.097
Beam Diameter (mm)	1	2914	2913.9	8.11	0.036
Square	3	87616	29205.3	81.32	0.000
Power (W)*Power (W)	1	44151	44151.2	122.94	0.000
Scanning Speed (mm/s)*Scanning Speed (mm/s)	1	8066	8066.0	22.46	0.005
Beam Diameter (mm)*Beam Diameter (mm)	1	34953	34953.2	97.32	0.000
2-Way Interaction	3	42611	14203.7	39.55	0.001
Power (W)*Scanning Speed (mm/s)	1	1509	1509.3	4.20	0.096
Power (W)*Beam Diameter (mm)	1	37652	37651.5	104.84	0.000
Scanning Speed (mm/s)*Beam Diameter (mm)	1	3450	3450.4	9.61	0.027
Error	5	1796	359.1		
Lack-of-Fit	3	1499	499.6	3.37	0.237
Pure Error	2	297	148.4		
Total	14	140673			

TABLE 5. ANOVA results for Kerf-down

Source	DF	Adj SS	Adj MS	F-Value	P-Value
Model	9	44110.2	4901.1	2.59	0.154
Linear	3	4717.5	1572.5	0.83	0.532
Power (W)	1	98.6	98.6	0.05	0.829
Scanning Speed (mm/s)	1	1291.3	1291.3	0.68	0.447
Beam Diameter (mm)	1	3327.6	3327.6	1.76	0.242
Square	3	35900.7	11966.9	6.31	0.037
Power (W)*Power (W)	1	13703.1	13703.1	7.23	0.043
Scanning Speed (mm/s)*Scanning Speed (mm/s)	1	9427.5	9427.5	4.97	0.076
Beam Diameter (mm)*Beam Diameter (mm)	1	11051.8	11051.8	5.83	0.061
2-Way Interaction	3	3491.9	1164.0	0.61	0.635
Power (W)*Scanning Speed (mm/s)	1	306.3	306.3	0.16	0.704
Power (W)*Beam Diameter (mm)	1	1582.4	1582.4	0.83	0.403
Scanning Speed (mm/s)*Beam Diameter (mm)	1	1603.2	1603.2	0.85	0.400
Error	5	9476.2	1895.2		
Lack-of-Fit	3	7747.7	2582.6	2.99	0.261
Pure Error	2	1728.5	864.2		
Total	14	53586.4			

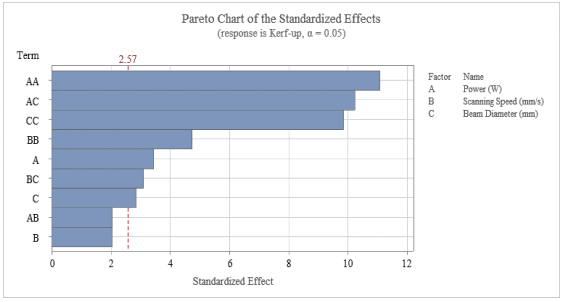

(a)

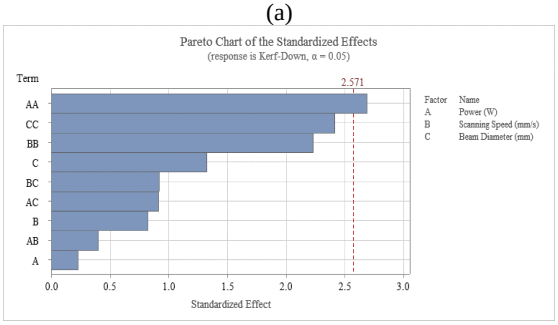

(b)

Figure 5. The Pareto chart for Kerf width at (a) top and (b) bottom surface

trends have been observed for kerf width at the bottom surface. The vertical axis of Figure 6 (a) and (b) is the magnitude of kerf width. As can be seen, the kerf-up width value is higher than the kerf-down value which shows the formation of kerf taper angle as shown in Figure 1.

Figure 7 shows the contour plot and surface plot of kerf width at the top surface. The interaction of process parameters shows that the kerf-up width decreases by increasing the laser power at constant scanning speed, then it increases and a saddle shape was observed as the surface response. The interaction of laser beam diameter with laser power shows that the kerf-up width decreases by simultaneously decreasing both the laser beam diameter and laser power and then it increases as shown in Figure 7 (c). The response surface is like a bowl-shaped surface which determines a local minimum at 90 W laser power and 0.6 mm laser beam diameter. The interaction of scanning speed with laser beam diameter shows that the effect of scanning speed is almost constant at low and high levels of laser beam diameter (0.2 mm and 1mm) while the kerf-up width increases at first and then decreases at 0.6 mm laser beam diameter. The shape of the response surface of the kerf-down width is similar to the kerf-up width. The formation of kerf at the top and bottom surfaces of the sheet are unwanted phenomena and finding the behavior of the process output is very difficult. The statistical analysis of kerf width helps to determine this sophisticated phenomenon.

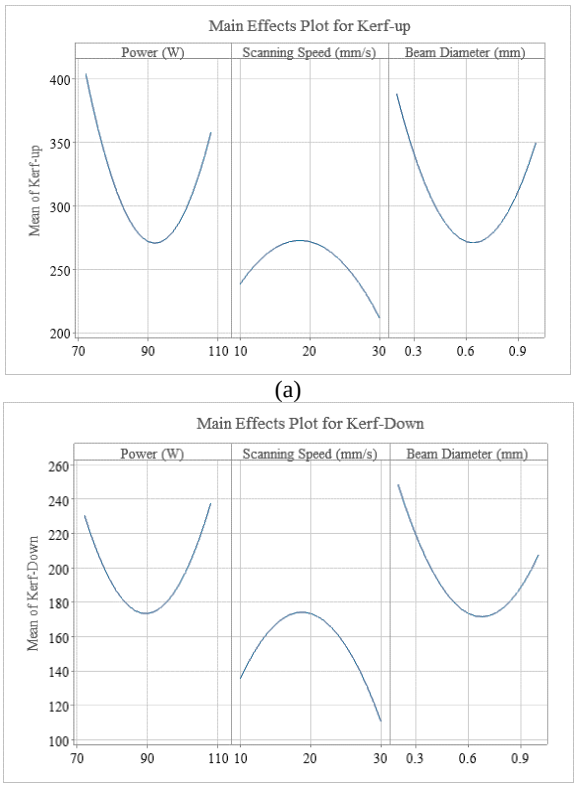

(a)

(b)

Figure 6. Main effect plot for kerf width at a) top and b) bottom surface

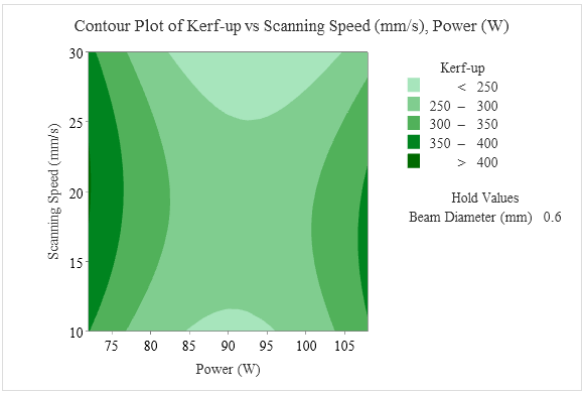

(a)

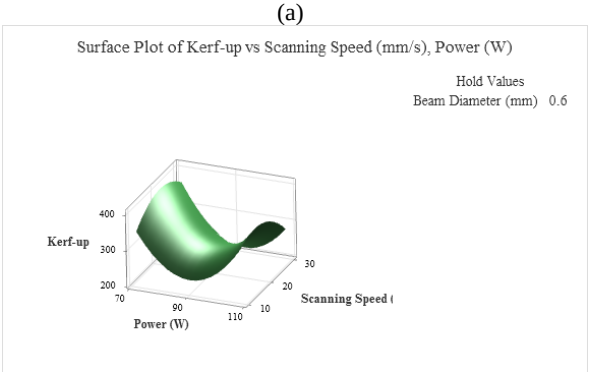

(b)

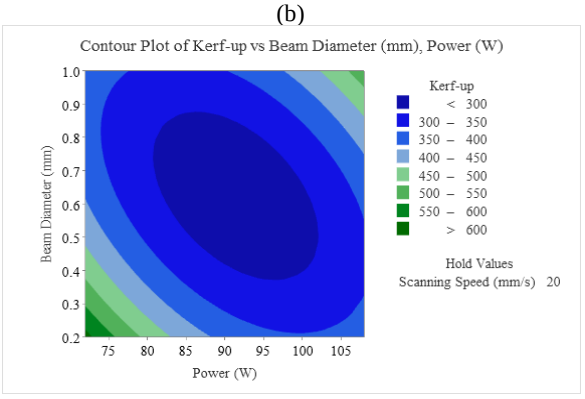

(c)

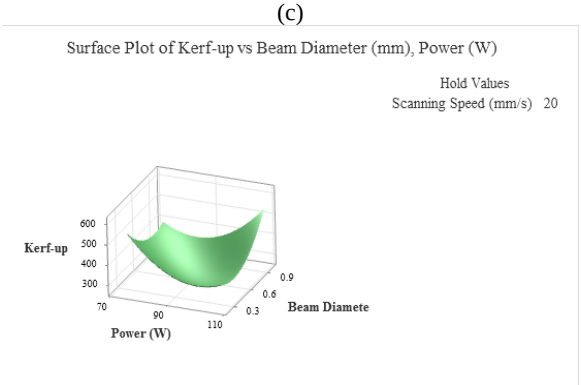

(d)

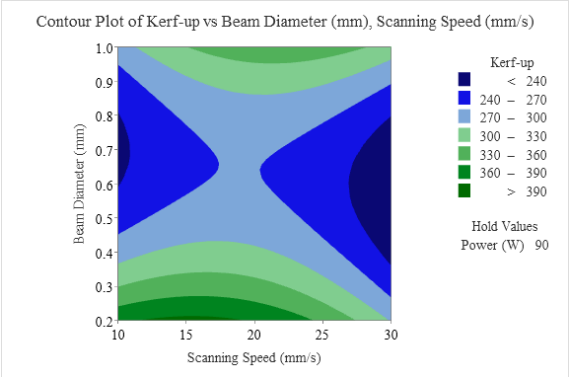

(e)

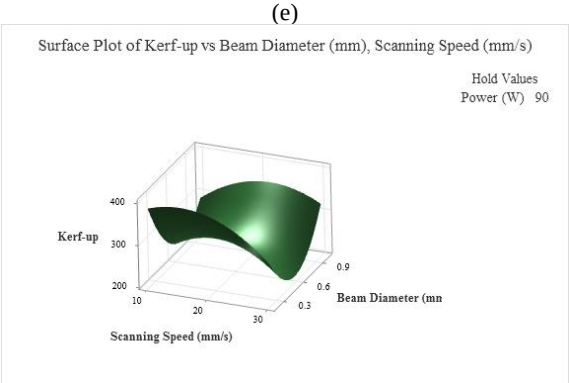

(f)

Figure 7. Contour plot and surface plot of kerf width at the top surface for the interaction of a, b) scanning speed with laser power, c, d) laser beam diameter with laser power, e, f) laser beam diameter with scanning speed

3. 3. Taper Angle Variation Analysis of variance had been carried out and the effect of process variables was determined. The taper angle can be predicted by Equation 5. Based on ANOVA results, the main effect plot is shown in Figure 8. The taper angle decreases by increasing the laser power. The taper angle increases at first and then it decreases by increasing the scanning speed. The taper angle decreases at first and then it increases by increasing the beam diameter. Comparing Figure 6 with Figure 8, that shows the scanning speed and laser beam diameter have similar trends in kerf width at the top and bottom surface and taper angle. But the laser power is different. Despite increasing the kerf width at the top and bottom surface, the taper angle decreases. Increasing the laser power causes a higher material removal rate (higher melting and evaporating rate) and in this condition, the surface roughness will increase due to higher energy absorption.

$$\begin{aligned} Taper\ Angle = {} & 11.39 - 0.146P + 0.112S - 12.93D \\ & + 0.000382P^2 - 0.00332S^2 \\ & + 2.20D^2 - 0.00000P \times S \\ & + 0.1095P \times D + 0.0239S \times D \end{aligned} \quad (5)$$

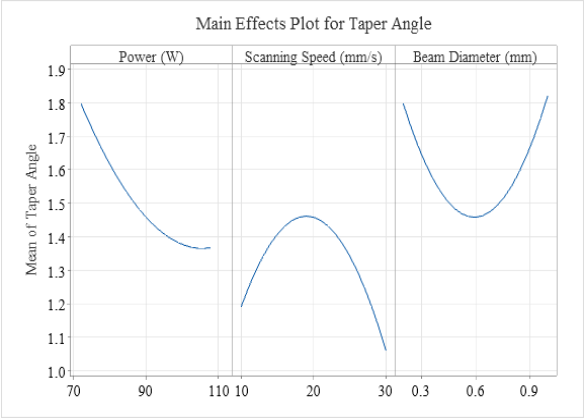

Figure 8. Main effect plot for taper angle

Figure 9 shows the contour plot and surface plot of the kerf taper angle. The results show that the taper angle increases at first then it decreases at different scanning speeds. Also, the taper angle decreases slightly by increasing the laser power. Maximum taper angle obtained at low laser power and moderate scanning speed. The taper angle decreases by increasing the laser power at a low beam diameter, but the taper angle increases by increasing the laser power at a high beam diameter. Minimum taper angle obtained at high laser power and low beam diameter. The interaction of laser beam diameter and scanning speed forms a saddle-shaped surface. Increasing the scanning speed increases at first, then it decreases. By increasing the beam diameter, the taper angle decreases at first, then it increases. Minimum taper angle obtained at high scanning speed and moderate beam diameter. The contour plot and surface plot show the complex interaction of the process variables and the minimum should be determined by optimization. Optimization by the Minitab software shows that the minimum bending angle will be obtained at high laser power (108W), high scanning speed (30 mm/s), and low beam diameter (0.2 mm) if the taper angle is the only target of optimization.

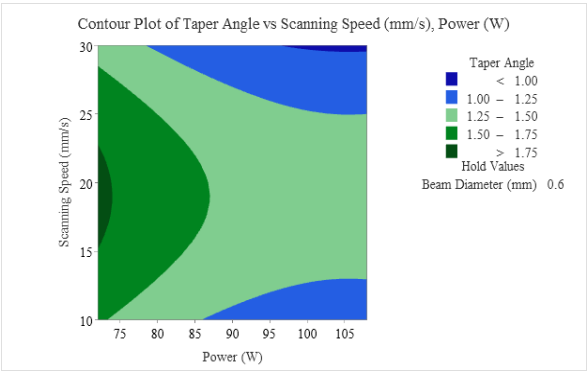

(a)

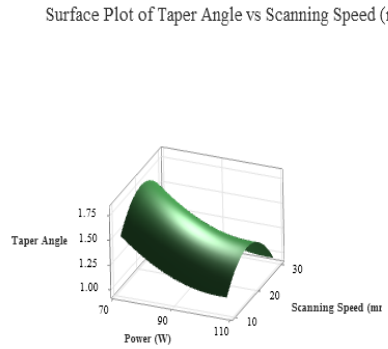

(b)

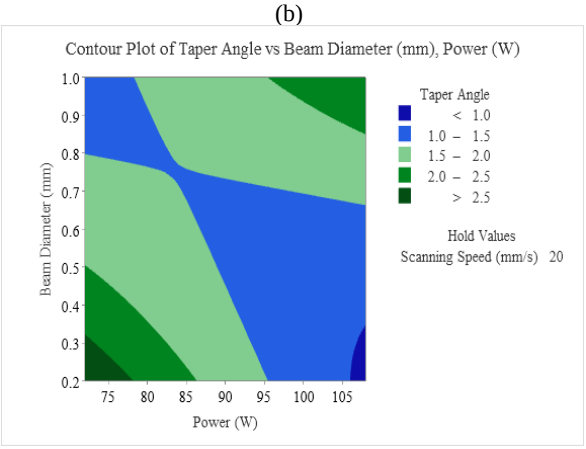

(c)

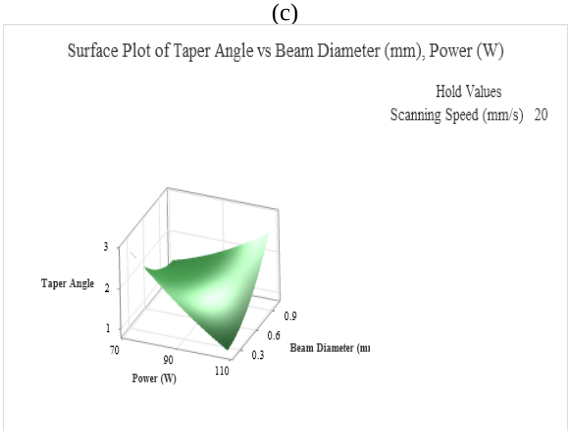

(d)

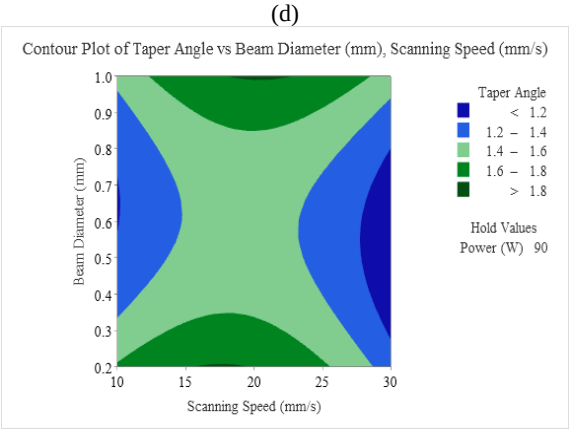

(e)

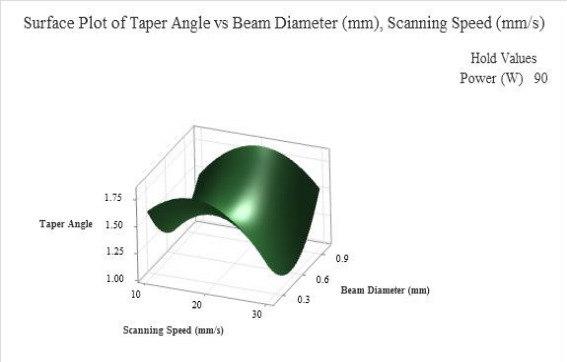

(f)

Figure 9. Contour plot and surface plot of kerf taper angle by a, b) scanning speed with laser power, c, d) laser beam diameter with laser power, e, f) laser beam diameter with scanning speed

At last, it should be noted that using RSM helps to interpret the results of statistical analysis better than the full-factorial design of experiments. In the full-factorial data analysis, the trend of variation should always be positive or negative (increasing or decreasing functions). But, as we can see in Figures 4, 6, and 8, the process output mostly increases at first, then it decreases or vice versa. So, using RSM can better predict the variation of the process output. While the number of experiments (15 experiments) is also lower than the full-factorial design (27 experiments). It should be noted that the data analysis by statistical tools helps the researchers to introduce a semi-empirical semi-analytical equation that is reliable in the range of the process parameters variation. In other words, regardless of the non-linear behavior of the process output, a quadratic equation can describe the trends of output change.

3. 4. Optimized Process Conditions The effect of process variables is complicated in laser cutting. The effect of each variable and the interaction of the process variables is discussed in the previous section. Finding the optimum condition needs special considerations. The taper angle is calculated according to the value of kerf width at the top and bottom surfaces. So, the minimum taper angle will not happen at the minimum kerf width at the top surface (kerf-up) and kerf width at the bottom surface (kerf-down). Figure 10 shows the condition of minimum kerf-up and kerf-down width. The results show that if the laser power was 88 W, the scanning speed was 30 mm/s, and the beam diameter was 1 mm, the minimum kerf-up and kerf-down width would be obtained. In these conditions, the kerf-up, kerf-down width, and kerf taper angle will be 215.7 µm, 109.5 µm, and 1.07 °, respectively. The average surface roughness Ra will be 1.23 µm which is a coarse surface roughness. The taper angle of the kerf will not be the minimum. Figure 11 shows the optimized condition for obtaining minimum

surface roughness and minimum kerf taper angle simultaneously. The optimized condition for minimum surface roughness and minimum kerf taper angle is 106.5 W laser power, 10 mm/s scanning speed, and 0.2 mm beam diameter. The surface roughness and kerf taper angle at optimized conditions will be 0.38 µm and 0.809 ° respectively. In this situation, the kerf-up and kerf-down width will be 383.7 and 258.8, respectively.

Different attitudes can be selected in the optimization of process variables. Minimizing all four parameters leads to a narrow kerf but the surface roughness will be coarse comparatively. One of the best choices for optimization is minimizing the kerf-up and kerf-down width and minimizing the surface roughness (Figure 12). The results show that the process variables should be set as 87 W laser power, 10 mm/s scanning speed and 0.54 mm beam diameter to optimize the surface roughness (0.570 µm), kerf-up width (250 µm) and kerf-down width (143 µm). In this condition, the taper angle will be 1.25°.

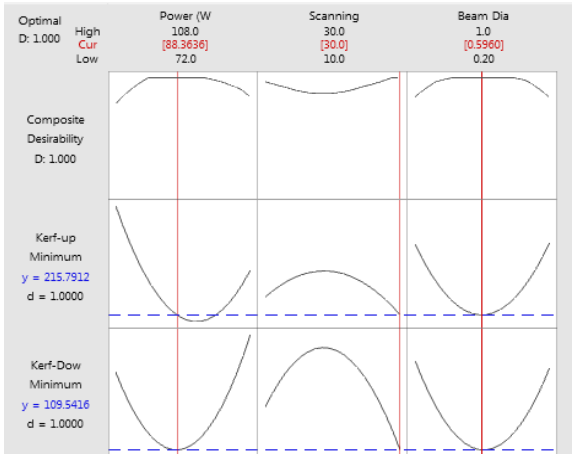

Figure 10. Optimized condition of kerf width at the top and bottom surfaces

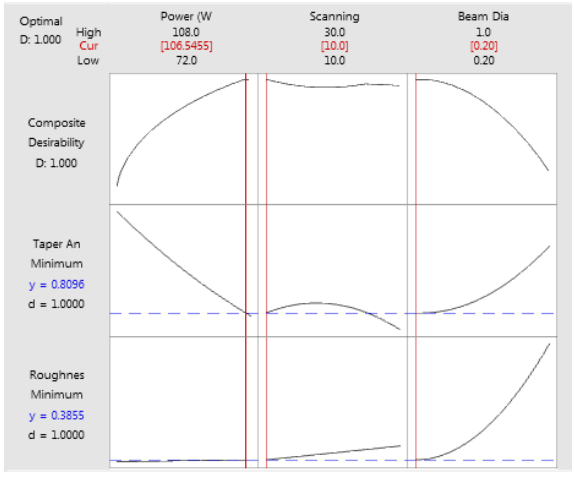

Figure 11. Optimized condition of surface roughness and kerf taper angle

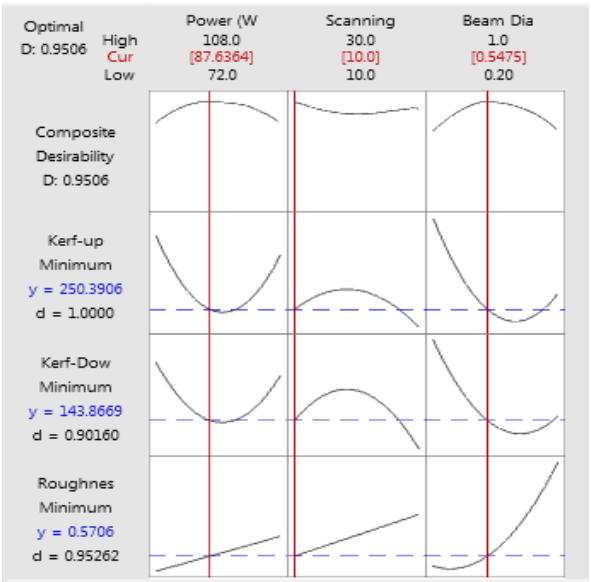

Figure 12. Optimized condition of surface roughness, kerf-up width, and kerf-down width

At the end, it should be noted that the attitude of this research was to find a regression equation between the process parameters and output parameters. ANOVA helps to identify the trend of variation and this was a cognitive process. So, no improvement existed to be discussed quantitatively. The main achievement of this article is finding the equations of output variables and determining the effect of the main and interactions of the process variables.

4. CONCLUSION

In this study, the laser cutting of thin PMMA sheets has been investigated using RSM. The analysis of variance has been utilized to investigate the effect of process variables and their interactions on surface roughness, kerf width, and taper angle. The results show that the beam diameter is the most influential process variable on surface roughness and minimum surface roughness will be obtained at 0.3 mm beam diameter. The minimum kerf-up and kerf-down width were obtained at about 90W laser power, 0.6 mm beam diameter, and 30 mm/s scanning speed. Increasing the laser power reduces the kerf taper angle of the cut surface and the minimum taper angle can be obtained at 0.6 mm beam diameter and 30 mm/s scanning speed. The surface roughness decreases by decreasing the laser power and scanning speed. Multi-objective optimization shows that the optimized condition for minimum surface roughness, kerf-up, and kerf-down width was obtained by setting the process parameters as 87 W laser power, 10 mm/s scanning speed, and 0.54 mm beam diameter.

5. REFERENCES

1. Li H, Fan Y, Kodzius R, Foulds IG. Fabrication of polystyrene microfluidic devices using a pulsed CO 2 laser system. Microsystem technologies. 2012;18:373-9. 10.1007/s00542-011-1410-z
2. Chen X, Li T, Zhai K, Hu Z, Zhou M. Using orthogonal experimental method optimizing surface quality of CO 2 laser cutting process for PMMA microchannels. The International Journal of Advanced Manufacturing Technology. 2017;88:2727-33. 10.1007/s00170-016-8887-7
3. Huang Y, Liu S, Yang W, Yu C. Surface roughness analysis and improvement of PMMA-based microfluidic chip chambers by CO2 laser cutting. Applied surface science. 2010;256(6):1675-8. 10.1016/j.apsusc.2009.09.092
4. Mosalman S, Rashahmadi S, Hasanzadeh R. The effect of tio2 nanoparticles on mechanical properties of poly methyl methacrylate nanocomposites (research note). International Journal of Engineering, Transactions B: Applications. 2017;30(5):807-13. 10.5829/idosi.ije.2017.30.05b.22
5. Choudhury IA, Shirley S. Laser cutting of polymeric materials: an experimental investigation. Optics & Laser Technology. 2010;42(3):503-8. 10.1016/j.optlastec.2009.09.006
6. Eltawahni H, Olabi A-G, Benyounis K. Effect of process parameters and optimization of CO2 laser cutting of ultra high-performance polyethylene. Materials & Design. 2010;31(8):4029-38. 10.1016/j.matdes.2010.03.035
7. Eltawahni H, Olabi A, Benyounis K, editors. Assessment and optimization of CO 2 laser cutting process of PMMA. AIP conference proceedings; 2011: American Institute of Physics. 10.1063/1.3552409
8. Ratnawati R, Wulandari R, Kumoro AC, Hadiyanto H. Response surface methodology for formulating PVA/starch/lignin biodegradable plastic. Emerging Science Journal. 2022;6(2):238-55. 10.28991/esj-2022-06-02-03
9. Safari M, Joudaki J, Ghadiri Y. A comprehensive study of the hydroforming process of metallic bellows: investigation and multi-objective optimization of the process parameters. International Journal of Engineering, Transactions B: Applications. 2019;32(11):1681-8. 10.5829/ije.2019.32.11b.19
10. Obinna AC, Mbah GO, Onoh MI. Optimization and process modeling of viscosity of oil based drilling muds. Journal of Human, Earth, and Future. 2021;2(4):412-23. 10.28991/hef-2021-02-04-09
11. Khoshaim AB, Elsheikh AH, Moustafa EB, Basha M, Showaib EA. Experimental investigation on laser cutting of PMMA sheets: Effects of process factors on kerf characteristics. journal of materials research and technology. 2021;11:235-46. 10.1016/j.jmrt.2021.01.012
12. Elsheikh AH, Deng W, Showaib EA. Improving laser cutting quality of polymethylmethacrylate sheet: experimental investigation and optimization. Journal of Materials Research and Technology. 2020;9(2):1325-39. 10.1016/j.jmrt.2019.11.059
13. Elsheikh AH, Shehabeldeen TA, Zhou J, Showaib E, Abd Elaziz M. Prediction of laser cutting parameters for polymethylmethacrylate sheets using random vector functional link network integrated with equilibrium optimizer. Journal of Intelligent Manufacturing. 2021;32:1377-88. 10.1007/s10845-020-01617-7
14. Yang C-B, Deng C-S, Chiang H-L. Combining the Taguchi method with artificial neural network to construct a prediction model of a CO 2 laser cutting experiment. The International Journal of Advanced Manufacturing Technology. 2012;59:1103-11. 10.1007/s00170-011-3557-2
15. Ninikas K, Kechagias J, Salonitis K. The impact of process parameters on surface roughness and dimensional accuracy during CO2 laser cutting of PMMA thin sheets. Journal of Manufacturing and Materials Processing. 2021;5(3):74. 10.3390/jmmp5030074
16. Kechagias JD, Ninikas K, Stavropoulos P, Salonitis K. A generalised approach on kerf geometry prediction during CO2 laser cut of PMMA thin plates using neural networks. Lasers in Manufacturing and Materials Processing. 2021;8(3):372-93. 10.1007/s40516-021-00152-4
17. Kechagias J, Ninikas K, Petousis M, Vidakis N, Vaxevanidis N. An investigation of surface quality characteristics of 3D printed PLA plates cut by CO2 laser using experimental design. Materials and Manufacturing Processes. 2021;36(13):1544-53. 10.1080/10426914.2021.1906892
18. Varsi AM, Shaikh AH. Experimental and statistical study on kerf taper angle during CO2 laser cutting of thermoplastic material. Journal of Laser Applications. 2019;31(3). 10.2351/1.5087846
19. Mushtaq RT, Wang Y, Rehman M, Khan AM, Mia M. State-of-the-art and trends in CO2 laser cutting of polymeric materials—a review. Materials. 2020;13(17):3839. 10.3390/ma13173839
20. Hashemzadeh M, Voisey K, Kazerooni M. The effects of low-frequency workpiece vibration on low-power CO 2 laser cutting of PMMA: an experimental investigation. The International Journal of Advanced Manufacturing Technology. 2012;63:33-40. https://doi.org/10.1007/s00170-011-3881-6
21. Safari M, Alves de Sousa R, Joudaki J. Recent advances in the laser forming process: A review. Metals. 2020;10(11):1472. 10.3390/met10111472
22. Safari M, Alves de Sousa R, Joudaki J. Comprehensive assessment of laser tube bending process by response surface methodology. steel research international. 2023;94(2):2200230. 10.1002/srin.202200230
23. Safari M, Rabiee AH, Joudaki J. Developing a Support Vector Regression (SVR) Model for Prediction of Main and Lateral Bending Angles in Laser Tube Bending Process. Materials. 2023;16(8):3251. 10.3390/ma16083251
24. Montgomery DC. Design and analysis of experiments: John wiley & sons; 2017.

Persian Abstract

چکیده

برش لیزری یک ابزار دقیق، قدرتمند و با هزینه پایین برای برش ورق های مختلف از چنس فلز و پلیمرها است. بررسی مقالات چاپ شده نشان می‌دهد که کیفیت برش (زبری سطح و هندسه شیار برش) یک پارامتر پیچیده است و روش‌های مرسوم نمی‌توانند کیفیت برش ورق‌های نازک پلیمرها را به خوبی توصیف کنند. ابزارهای آماری می توانند برای تفسیر تأثیر متغیرهای فرآیند مورد استفاده قرار گیرند. در این مقاله به بررسی برش لیزری پلی متیل متاکریلات (PMMA) به صورت تجربی پرداخته خواهد شد. اثر متغیرهای فرآیند برش لیزری شامل سرعت اسکن، توان لیزر و قطر پرتو لیزر بر روی عرض شیار برش و زبری سطح با کمک روش سطح پاسخ مورد بررسی قرار گرفت. نتایج نشان داد که افزایش توان لیزر منجر به افزایش زبری سطح و کاهش زاویه مخروطی شدن شیار می‌شود، در حالی که عرض شیار برش در سطح بالا و سطح پایین ورق، ابتدا کاهش و سپس افزایش می‌یابد (برای توان لیزر بالاتر از ۹۰ وات). همچنین افزایش سرعت اسکن باعث افزایش زبری سطح می شود در حالی که زاویه مخروطی و پهنای عرض شیار برش در سطح بالا و سطح پایین ابتدا افزایش یافته و سپس کاهش می یابد. با افزایش قطر پرتو لیزر، زبری سطح افزایش می یابد، در حالی که زاویه مخروطی و عرض شیار برش در سطح بالا و سطح پایین ابتدا کاهش و سپس افزایش می یابد. بررسی اثر متغیرهای فرآیند اصلی و برهمکنش‌های آنها نشان داد که یافتن شرایط بهینه پارامترهای فرآیند کار سختی است و باید از روشهای بهینه‌سازی چند هدفه برای یافتن حداقل زبری سطح و عرض شیار برش استفاده نمود.